LIQUEFACTION RESISTANCE OF SOILS FROM SHEAR-WAVE VELOCITY

By Ronald D. Andrus,[1] Associate Member, ASCE,
and Kenneth H. Stokoe II,[2] Member, ASCE

ABSTRACT: A simplified procedure using shear-wave velocity measurements for evaluating the liquefaction resistance of soils is presented. The procedure was developed in cooperation with industry, researchers, and practitioners and evolved from workshops in 1996 and 1998. It follows the general format of the Seed-Idriss simplified procedure based on standard penetration test blow count and was developed using case history data from 26 earthquakes and >70 measurement sites in soils ranging from fine sand to sandy gravel with cobbles to profiles including silty clay layers. Liquefaction resistance curves were established by applying a modified relationship between the shear-wave velocity and cyclic stress ratio for the constant average cyclic shear strain suggested by R. Dobry. These curves correctly predicted moderate to high liquefaction potential for >95% of the liquefaction case histories and are shown to be consistent with the standard penetration test based curves in sandy soils. A case study is provided to illustrate application of the procedure. Additional data are needed, particularly from denser soil deposits shaken by stronger ground motions, to further validate the simplified procedure.

INTRODUCTION

Evaluation of the liquefaction resistance of soils is an important step in many geotechnical investigations in earthquake-prone regions. The procedure widely used in the United States and throughout much of the world for evaluating soil liquefaction resistance is termed the "simplified procedure." This simplified procedure was originally developed by Seed and Idriss (1971) using blow counts from the standard penetration test (SPT) correlated with a parameter called the cyclic stress ratio that represents the cyclic loading on the soil. Since 1971, this procedure has been revised and updated (Seed 1979; Seed and Idriss 1982; Seed et al. 1983, 1985; Youd et al. 1997). In the mid-1980s, a parallel procedure based on the cone penetration test (CPT) was introduced by Robertson and Campanella (1985), which also has been revised and updated (Seed and de Alba 1986; Stark and Olson 1995; Olsen 1997; Robertson and Wride 1998).

A promising alternative, or supplement, to the penetration-based approaches is provided by in situ measurements of small-strain shear-wave velocity V_S. The use of V_S as an index of liquefaction resistance is soundly based because both V_S and liquefaction resistance are similarly influenced by many of the same factors (e.g., void ratio, state of stress, stress history, and geologic age). Some advantages of using V_S are that (Dobry et al. 1981; Seed et al. 1983; Stokoe et al. 1988a; Tokimatsu and Uchida 1990) (1) the measurements are possible in soils that are hard to sample, such as gravelly soils where penetration tests may be unreliable; (2) measurements can also be performed on small laboratory specimens, allowing direct comparisons between laboratory and field behavior; (3) V_S is a basic mechanical property of soil materials, directly related to small-strain shear modulus G_{max} by

$$G_{max} = \rho V_S^2 \tag{1}$$

where ρ = mass density of soil; (4) G_{max}, or V_S, is normally a required property in earthquake site response and soil-structure interaction analyses; and (5) V_S can be measured by the spectral-analysis-of-surface-waves (SASW) technique at sites where borings may not be permitted, such as capped landfills, sites that extend for great distances where rapid evaluation is required, and hard-to-sample sites composed of gravels, cobbles, and even boulders.

Three concerns when using V_S to evaluate liquefaction resistance are that (1) no samples are routinely obtained as part of the testing procedure for soil classification and identification of nonliquefiable materials; (2) thin, low V_S strata may not be detected if the measurement interval is too large [U.S. Bureau of Reclamation (USBR) 1989; Boulanger et al. 1997]; and (3) measurements are made at small strains, whereas pore-water pressure buildup and liquefaction are medium- to high-strain phenomena (Jamiolkowski and Lo Presti 1990; Teachavorasinskun et al. 1994; Roy et al. 1996). This third concern can be significant for cemented soils, because small-strain measurements are highly sensitive to weak interparticle bonding that is eliminated at medium and high strains. It also can be significant in silty soils above the water table where negative pore-water pressures can increase V_S.

Over the past 20 years, numerous studies have been conducted to investigate the relationship between V_S and liquefaction resistance. These studies involved field performance observations [e.g., Stokoe and Nazarian (1985), Robertson et al. (1992), Kayen et al. (1992), and Andrus and Stokoe (1997)], penetration-V_S correlations [e.g., Seed et al. (1983) and Lodge (1994)], analytical investigations [e.g., Bierschwale and Stokoe (1984) and Stokoe et al. (1988b)], and laboratory tests [e.g., Dobry et al. (1981), de Alba et al. (1984), and Tokimatsu and Uchida (1990)]. Several of the liquefaction evaluation procedures developed from these studies follow the general format of the Seed-Idriss simplified procedure, where V_S is corrected to a reference overburden stress and correlated with the cyclic stress ratio. Nearly all were developed with limited or no field performance data.

Summarized in this paper is the procedure originally proposed in the workshop paper by Andrus and Stokoe (1997) and subsequently updated in the project report by Andrus et al. (1999). The procedure is based on field performance data from 26 earthquakes and in situ V_S measurements from >70 sites. Suggestions from two technical workshops have been incorporated into the procedure. The first workshop was held on January 4–5, 1996, in Salt Lake City, and was sponsored by the National Center for Earthquake Engineering Research (NCEER). The second workshop was held on August 14–15, 1998, also in Salt Lake City, and was sponsored by the Multidisciplinary Center for Earthquake Engineering Research

[1]Asst. Prof., Dept. of Civ. Engrg., Clemson Univ., Clemson, SC 29634; formerly, Res. Civ. Engr., Nat. Inst. of Standards and Technol., Gaithersburg, MD 20899.

[2]Jennie C. and Milton T. Graves Chair, Dept. of Civ. Engrg., Univ. of Texas at Austin, Austin, TX 78712.

Note. Discussion open until April 1, 2001. To extend the closing date one month, a written request must be filed with the ASCE Manager of Journals. The manuscript for this paper was submitted for review and possible publication on September 17, 1999. This paper is part of the ***Journal of Geotechnical and Geoenvironmental Engineering***, Vol. 126, No. 11, November, 2000. ©ASCE, ISSN 1090-0241/00/0011-1015–1025/$8.00 + $.50 per page. Paper No. 21881.

(MCEER), formally NCEER, and the National Science Foundation. These workshops are herein called the 1996 NCEER and 1998 MCEER workshops.

EVALUATION PROCEDURE

The evaluation procedure requires the calculation of three parameters: (1) The level of cyclic loading on the soil caused by the earthquake, expressed as a cyclic stress ratio; (2) stiffness of the soil, expressed as an overburden stress-corrected shear-wave velocity; and (3) resistance of the soil to liquefaction, expressed as a cyclic resistance ratio. Each parameter is discussed below.

Cyclic Stress Ratio *CSR*

The cyclic stress ratio, τ_{av}/σ'_v, at a particular depth in a level soil deposit can be expressed (Seed and Idriss 1971):

$$CSR = \frac{\tau_{av}}{\sigma'_v} = 0.65 \left(\frac{a_{\max}}{g}\right)\left(\frac{\sigma_v}{\sigma'_v}\right) r_d \tag{2}$$

where τ_{av} = average equivalent uniform cyclic shear stress caused by the earthquake and is assumed to be 0.65 of the maximum induced stress; $a_{\max}$ = peak horizontal ground surface acceleration; g = acceleration of gravity; σ'_v = initial effective vertical (overburden) stress at the depth in question; σ_v = total overburden stress at the same depth; and r_d = shear stress reduction coefficient to adjust for the flexibility of the soil profile.

Values of r_d are commonly estimated from the chart by Seed and Idriss (1971), using the average curve shown in Fig. 1. Their average curve was determined analytically using a variety of earthquake motions and soil conditions. Revised average r_d values have been proposed by Idriss (1999) based on the analytical work by Golesorkhi (1989). Unlike the original r_d values, these revised r_d values are magnitude dependent. As shown in Fig. 1, the revised r_d curve for moment magnitude $M_W = 7.5$ is almost identical to the average curve published by Seed and Idriss (1971).

Stress-Corrected Shear-Wave Velocity

Shear-wave velocities can be measured in situ by several seismic tests including cross hole, downhole, seismic cone penetrometer, suspension logger, and SASW. A review of these test methods is given in Woods (1994). Their accuracy can be sensitive to procedural details, soil conditions, and interpretation techniques.

One important factor influencing V_S is the state of stress in soil (Hardin and Drnevich 1972). Laboratory test results (Roesler 1979; Stokoe et al. 1985; Belloti et al. 1996) show that the velocity of a propagating shear wave depends equally on principal stresses in the direction of wave propagation and particle motion. Thus, V_S measurements made with wave propagation or particle motion in the vertical direction can be related by the following empirical relationship:

$$V_S = A(\sigma'_v)^m(\sigma'_h)^m \tag{3}$$

where A = parameter that depends on the soil structure; σ'_h = initial effective horizontal stress at the depth in question; and m = stress exponent with a value of about 0.125.

Following the traditional procedures for correcting SPT blow count and CPT tip resistances to account for overburden stress, one can correct V_S to a reference overburden stress by (Sykora 1987; Robertson et al. 1992)

$$V_{S1} = V_S C_V = V_S \left(\frac{P_a}{\sigma'_v}\right)^{0.25} \tag{4}$$

where V_{S1} = overburden stress-corrected shear-wave velocity; C_V = factor to correct measured shear-wave velocity for overburden pressure; P_a = reference stress of 100 kPa or about atmospheric pressure; and σ'_v = initial effective overburden stress (kPa). A maximum C_V value of 1.4 is generally applied to V_S data at shallow depths, similar to the SPT and CPT procedures. In using (4), it is implicitly assumed from the relationship given in (3) that the initial effective horizontal stress σ'_h is a constant factor of the effective overburden stress. The factor, generally referred to as K'_0, is assumed to be approximately 0.5 at natural, level-ground sites where liquefaction has occurred or is likely to occur. Also, in applying (4), it is implicitly assumed that V_S is measured with both particle motion and wave propagation polarized along principal stress directions and one of those directions is vertical.

Cyclic Resistance Ratio *CRR*

The value of *CSR* separating liquefaction and nonliquefaction occurrences for a given V_{S1}, or corrected penetration resistance, is called the cyclic resistance ratio *CRR*. R. Dobry (personal communication, January 6, 1996) derived a relationship between *CSR* and V_{S1} for a constant average cyclic shear strain using (1) and

$$\gamma_{av} = \frac{\tau_{av}}{(G)_{\gamma_{av}}} \tag{5}$$

where γ_{av} = average peak shear strain during a cyclic stress-controlled test of uniform cyclic shear stress τ_{av}; and $G_{\gamma_{av}}$ = secant shear modulus at γ_{av} during the same cyclic test. By combining (1) and (5), the following relationship is obtained:

$$CSR = \frac{\tau_{av}}{\sigma'_v} = f(\gamma_{av})V_{S1}^2 \tag{6}$$

where $f(\gamma_{av})$ = function of γ_{av}. Because *CSR* equals *CRR* at the point separating liquefaction and nonliquefaction, (6) provides an analytical basis for establishing the *CRR*-V_{S1} curves at low values of V_{S1} (say $V_{S1} \leq 125$ m/s) and extending them to zero at $V_{S1} = 0$.

Andrus and Stokoe (1997) modified (6) to

$$CRR = \left\{ a\left(\frac{V_{S1}}{100}\right)^2 + b\left(\frac{1}{V^*_{S1} - V_{S1}} - \frac{1}{V^*_{S1}}\right)\right\} MSF \tag{7}$$

where V^*_{S1} = limiting upper value of V_{S1} for cyclic liquefaction occurrence; a and b = curve fitting parameters; and *MSF* = magnitude scaling factor to account for the effect of earthquake magnitude. The first term in (7) is a form of (6), assuming $f(\gamma_{av})$ is independent of initial effective confining pressure

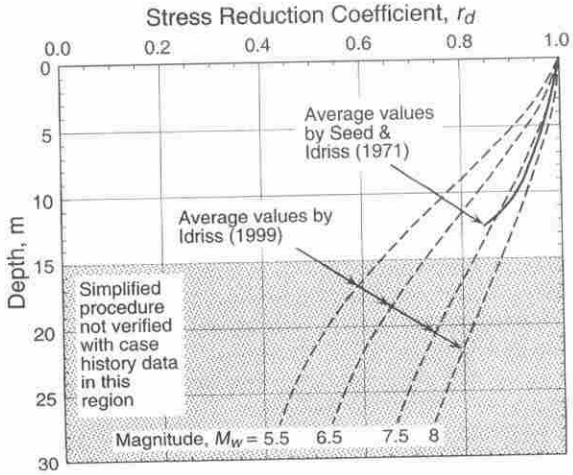

FIG. 1. Shear Stress Reduction Factor Used to Adjust for Flexibility in Soil Profiles During Earthquake Shaking

and pore-water pressure buildup. The second term is a hyperbola with a small value at low values of V_{S1} and a very large value as V_{S1} approaches V^*_{S1}.

The assumption of a limiting upper value of V_{S1} is equivalent to the assumption commonly made in the SPT- and CPT-based procedures dealing with clean sands, where liquefaction is considered not possible above a corrected blow count of about 30 (Seed et al. 1985) and corrected tip resistance of about 160 (Robertson and Wride 1998). Upper limits for V_{S1} and penetration resistance are explained by the tendency of dense soils to exhibit dilative behavior at large strains, causing negative pore-water pressures. Although it is possible in a dense soil to generate pore-water pressures close to the confining stress if large cyclic strains or many cycles are applied, the amount of water expelled during reconsolidation is dramatically less for dense soils than for loose soils. As explained by Dobry (1989), in dense soils, settlement is insignificant and no sand boils or failure take place because of the small amount of water expelled. This is important because the definition of liquefaction used to classify the field behavior here, as well as in the penetration-based procedures, is based on surface manifestations.

The magnitude scaling factor is traditionally applied to *CRR*, rather than the cyclic loading parameter *CSR*, and equals 1.0 for earthquakes with a magnitude of 7.5. For magnitudes other than 7.5, Fig. 2 presents magnitude scaling factors developed by various investigators. The 1996 NCEER workshop (Youd et al. 1997) recommended a range of factors that can be represented by

$$MSF = \left(\frac{M_w}{7.5}\right)^n \tag{8}$$

where M_w = moment magnitude; and n = exponent. Moment magnitude is the scale most commonly used for engineering applications and is preferred for liquefaction resistance calculations (Youd et al. 1997). The lower bound for the range of *MSF*s recommended by the 1996 NCEER workshop is defined with $n = -2.56$ (I. M. Idriss, personal communication, October, 1995). The upper bound of the recommended range is defined with $n = -3.3$ (Andrus and Stokoe 1997) for earthquakes with magnitudes ≤7.5. Magnitude scaling factors defined by (8) and average r_d values originally proposed by Seed and Idriss (1971) should be used together when applying (2) and (7).

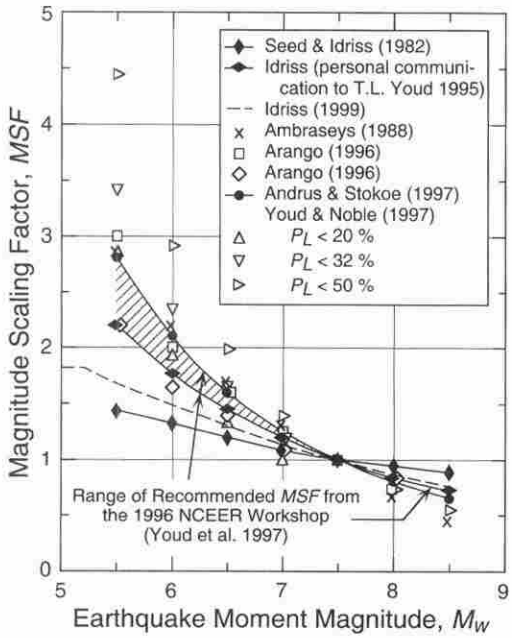

FIG. 2. Magnitude Scaling Factors Derived by Various Investigators and Range Recommended by 1996 NCEER Workshop [Modified from Youd et al. (1997)]

More recently, Idriss (1999) proposed revised *MSF*s defined by

$$MSF = 6.9 \exp\left(\frac{-M_w}{4}\right) - 0.06, \quad \text{for } M_w > 5.2 \tag{9a}$$

$$MSF = 1.82, \quad \text{for } M_w \leq 5.2 \tag{9b}$$

Magnitude scaling factors defined by (9) and revised r_d proposed by Idriss (1999) should be used together when applying (2) and (7). The difference in the two proposed *MSF* and r_d relationships is not significant for earthquakes with magnitudes of about 7–7.5 (Andrus et al. 1999), the range of the majority of the V_S case history data.

CASE HISTORY DATA

Shear-wave velocity measurements have been performed at many liquefaction sites. A summary of >70 sites (139 test arrays) and 26 earthquakes that have been studied by various investigators is given in Andrus et al. (1999). Table 1 presents a list of these 26 earthquakes, with the soil types associated with each case history. Pertinent characteristics of the case history data are described in more detail below.

Andrus et al. (1999) defined a case history as an earthquake and a test array. A test array is defined as the two boreholes used for cross-hole measurements, the borehole and source used for downhole measurements, the cone sounding and source used for seismic cone measurements, the borehole used for suspension logger measurements, or the line of receivers used for SASW measurements. By combining the 139 test arrays and 26 earthquakes, a total of 225 case histories were obtained, with 149 from the United States, 36 from Taiwan, 34 from Japan, and 6 from China.

The distribution of case histories with earthquake magnitude and liquefaction occurrence is presented in Fig. 3(a). When magnitude scales other than M_w were reported, they were converted to M_w using the relationship adopted by the 1996 NCEER workshop (Youd et al. 1997). The occurrence of liq-

TABLE 1. Earthquakes Used to Establish *CRR*-V_{S1} Curves

Earthquake (1)	M_w (2)	NUMBER OF CASE HISTORIES BY FINES CONTENT: Sands and Silts ≤5% (3)	Sands and Silts 6–34% (4)	Sands and Silts ≥35% (5)	Gravels ≤5% (6)	Gravels 6–34% (7)
1906 San Francisco, Calif.	7.7	—	4	4	4	—
1957 Daly City, Calif.	5.3	3	2	—	—	—
1964 Niigata, Japan	7.5	4	—	—	—	—
1975 Haicheng, China	7.3	—	—	6	—	—
1979 Imperial Valley, Calif.	6.5	—	9	2	—	—
1980 Chiba-ibaragi, Japan	5.9	—	1	1	—	—
1981 Westmorland, Calif.	5.9	—	9	2	—	—
1983 Borah Peak, Idaho	6.9	—	—	—	17	1
1985 Chiba-ibaragi, Japan	6.0	—	1	1	—	—
1986 Event LSST2, Taiwan	5.3	—	—	4	—	—
1986 Event LSST3, Taiwan	5.5	—	—	4	—	—
1986 Event LSST4, Taiwan	6.6	—	—	4	—	—
1986 Event LSST6, Taiwan	5.4	—	—	4	—	—
1986 Event LSST7, Taiwan	6.6	—	—	4	—	—
1986 Event LSST8, Taiwan	6.2	—	—	4	—	—
1986 Event LSST12, Taiwan	6.2	—	—	4	—	—
1986 Event LSST13, Taiwan	6.2	—	—	4	—	—
1986 Event LSST16, Taiwan	7.6	—	—	4	—	—
1987 Chiba-toho-oki, Japan	6.5	—	1	—	—	—
1987 Elmore Ranch, Calif.	5.9	—	9	2	—	—
1987 Superstition Hills, Calif.	6.5	—	9	2	—	—
1989 Loma Prieta, Calif.	7.0	19	30	14	4	—
1993 Kushiro-oki, Japan	8.3	1	1	—	—	—
1993 Hokkaido-nansei, Japan	8.3	—	2	1	1	—
1994 Northridge, Calif.	8.3	—	3	—	—	—
1995 Hyogo-ken Nanbu, Japan	6.9	1	9	—	—	9

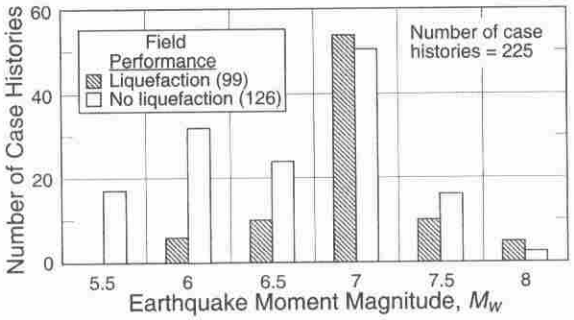

(a) Liquefaction Occurrence and Earthquake Magnitude

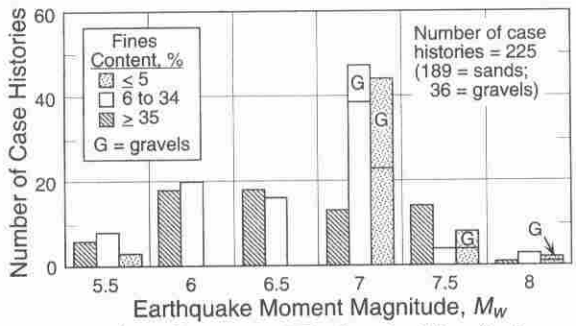

(b) Fines Content and Earthquake Magnitude

FIG. 3. Distribution of 225 Case Histories Based on Field Performance and Fines Content for Different Earthquake Magnitudes

uefaction was based on the appearance of surface evidence, such as sand boils, ground cracks and fissures, and ground settlement. At five sites the assessment of liquefaction or nonliquefaction occurrence was supported by pore-water pressure measurements. In addition, liquefaction occurrence was assigned (in this paper) to the Treasure Island, Calif., fire station cases, where the strong ground motion records from the 1989 Loma Prieta earthquake exhibit a sudden drop at about 15 s and small motion afterward (Idriss 1990), indicating liquefaction (de Alba et al. 1994). Of the 225 case histories, 99 were liquefaction case histories and 126 were nonliquefaction case histories.

Values of V_S reported by the investigators were used directly. Depending on the test method, in situ V_S measurements may be reported at discrete depths or for continuous intervals. When velocities were reported for continuous intervals, as is typically the case for downhole, seismic cone, suspension logger, and SASW measurements, the depth to the center of each interval was assumed. Thus, if the reported V_S profile had 10 velocity layers, it was assumed that the profile consisted of 10 "measurements" with depths at the center of each layer. Only the cross-hole measurements made with shear waves having particle motion in the vertical direction were used. Cross-hole measurements near the critical layer boundary that seemed high, and could represent refracted waves, were not included in the average. Some V_S values were from measurements performed before the earthquake, others followed the earthquake. No adjustments were made to compensate for changes in soil density and V_S due to ground shaking.

The layer of soil most likely to liquefy at a site, or the critical layer, was the layer of nonplastic soil below the ground-water table where values of V_{S1} and penetration resistance were generally the least and *CSR* relative to V_{S1} was the greatest. In Fig. 3(b), the distribution of case histories with earthquake magnitude, predominate soil type (gravel, sand, or silt) and average fines content (silt and clay) is presented. Of the 225 case histories, 28 were for sands with fines content $FC \leq 5\%$, 90 for sands with $FC = 6$–34%, 71 for sands and

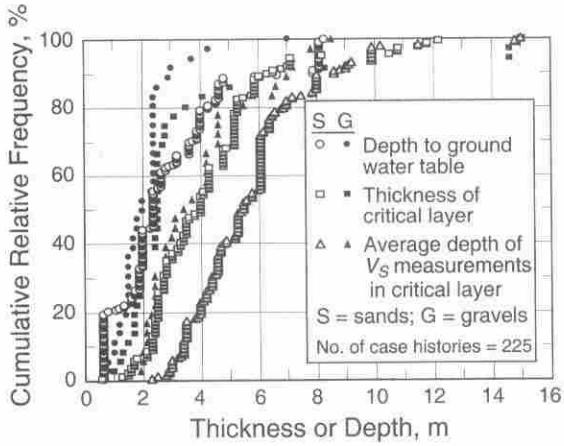

FIG. 4. Cumulative Relative Frequency of Case History Data by Thickness of Critical Layer, Average Depth of V_S Measurements in Critical Layer, and Depth to Ground-Water Table

silts with $FC \geq 35\%$, 26 for gravels with $FC \leq 5\%$, and 10 for gravels with $FC = 6$–34%. From the cumulative relative frequency distributions presented in Fig. 4, about 90% of the case histories had a critical layer thickness <7 m, average measurement depth <8 m, and water table depth <4 m. Overall, the gravel case histories exhibit smaller layer thicknesses and shallower measurement depths than do the sand and silt case histories.

About 70% of the case histories were for natural soil deposits, with many formed by alluvial processes. The other 30% were for hydraulic or dumped fills. Eight of the fills had been densified by soil improvement techniques. At least 85% of the case histories were for soils of Holocene age (<10,000 years). Although the ages of the other 15% were unknown, they were believed to be also of Holocene age.

Values of σ_v and σ'_v were estimated using soil densities reported by the investigators. When no densities were reported, typical values for soils with similar grain size, penetration, and velocity characteristics were assumed. In most instances, the assumed densities were 1.76 Mg/m^3 for soils above the water table and 1.92 Mg/m^3 for soils below the water table.

Because many published attenuation relationships between a_{max} and source distance are based on peak acceleration values obtained from ground motion records for two horizontal directions (sometimes referred to as the randomly oriented horizontal component), the geometric mean (square root of the product) of the two peak values was used. Use of the geometric mean is consistent with the development of the SPT-based procedure (Youd et al. 1997).

Values of V_{S1} and *CSR* were first calculated for each measurement depth within the critical layer and then averaged. In the calculations, each site was assumed to be level ground. Values of C_V used to correct measured shear-wave velocities ranged from 1.4 to 0.9 for most of the data. About 80% of the case histories have two to seven values on average.

LIQUEFACTION EVALUATION CHARTS

In the process of developing the liquefaction evaluation charts, all case history data were initially plotted on the same chart. This aggregation was accomplished through an adjustment procedure; that is, the *CSR* values in each case history were adjusted to an earthquake with $M_w = 7.5$ by dividing by (8) with $n = -2.56$. As done in penetration evaluation procedures, the sandy soil case histories were separated into three categories: (1) Sands with average $FC \leq 5\%$; (2) sands with average $FC = 6$–34%; and (3) sands and silts with average $FC \geq 35\%$. For consistency, the gravelly soil case histories also were divided into the same three categories based on fines

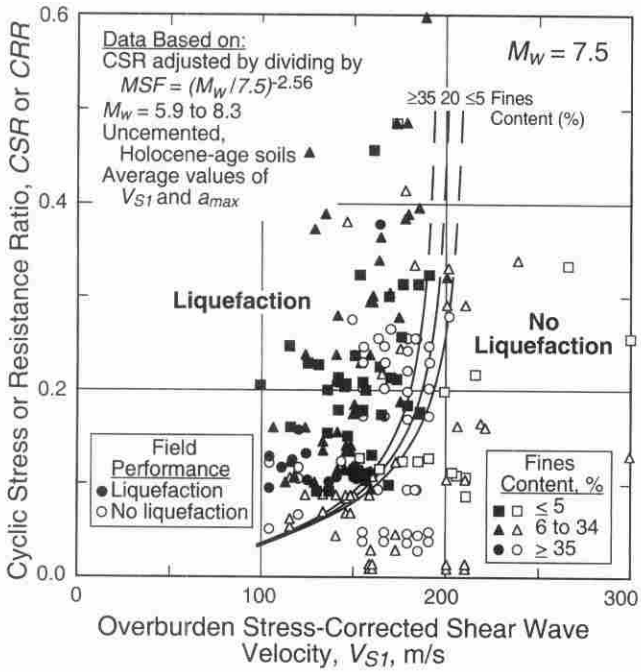

FIG. 5. Curves Recommended for Calculation of *CRR* from V_{S1} Measurements in Sands and Gravels along with Case History Data Based on Lower-Bound Values of *MSF* for Range Recommended by 1996 NCEER Workshop (Youd et al. 1997) and r_d Developed by Seed and Idriss (1971)

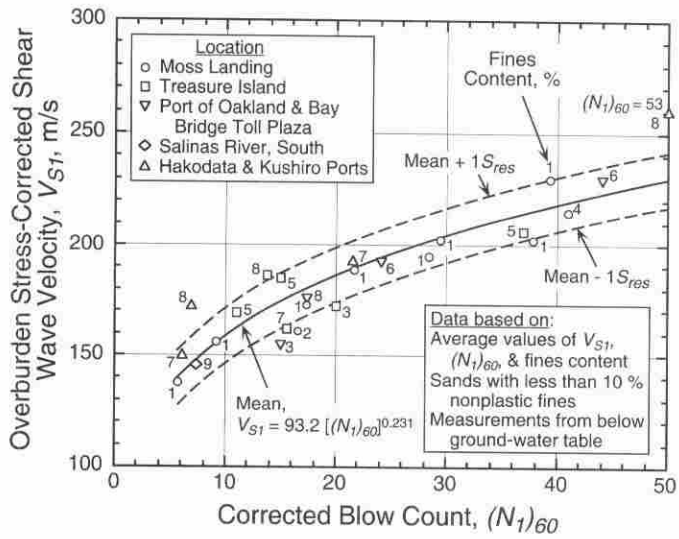

FIG. 6. Relationship between V_{S1} and $(N_1)_{60}$ for Uncemented, Holocene-Age Sands with <10% Nonplastic Fines from Case History Data

content. However, no case histories exist in the database with gravel having $FC \geq 35\%$. All data are plotted in Fig. 5 along with the proposed CRR-V_{S1} curves. Development of these curves is discussed below.

Limiting Upper Value of V_{S1} in Sandy Soils

As shown in Fig. 5, CSR values above about 0.35 are limited in the case history data. Thus, current estimates of V_{S1}^* rely, in part, on penetration-V_S correlations and, in part, on the data trend in Fig. 5. Furthermore, the penetration-V_S correlations are strongly biased toward measurements in sandy soils, because these types of measurements in gravelly and cobbly soils are still in the early application stage.

In the SPT-based procedure, a corrected blow count $(N_1)_{60}$ of 30 is assumed as the limiting upper value for cyclic liquefaction occurrence in sands with ≤5% silt and clay (Seed et al. 1985). The correlation by Ohta and Goto (1978) modified to a blow count with a theoretical free-fall energy of 60% (Seed et al. 1985) suggested equivalent V_{S1} values of 207 m/s for Holocene sands, assuming that a depth of 10 m is equivalent to an effective overburden stress of 100 kPa. The stress-corrected cross-hole measurements compiled by Sykora (1987) for Holocene sands and nonplastic silty sands below the ground-water table, with $(N_1)_{60}$ between 25 and 35, exhibit an average V_{S1} value of 206 m/s and standard deviation of 41 m/s. Finally, the case history data in this study were used to investigate the V_{S1} and $(N_1)_{60}$ relationship for well-documented sand layers with <10% fines. These data are presented in Fig. 6 along with the best-fit relationship that can be expressed

$$V_{S1} = B_1[(N_1)_{60}]^{B_2} \tag{10}$$

where $B_1 = 93.2 \pm 6.5$ and $B_2 = 0.231 \pm 0.022$ for soils with fines content <10% and with V_{S1} in meters per second and $(N_1)_{60}$ in blows/0.3 m. The plotted data exhibit a mean V_{S1} value of 204 m/s at a $(N_1)_{60}$ value of 30 and residual standard deviation S_{res} of 12 m/s.

From these estimates, a V_{S1} value of 210 m/s is assumed equivalent to a $(N_1)_{60}$ value of 30 in clean sands (≤5% fines). A value of 210 m/s for cyclic liquefaction occurrence at $CSR = 0.6$ is less than the general consensus value of 230 m/s suggested at the 1998 MCEER workshop. As a result, Fig. 6 was added specifically to provide additional evidence to support the use of 210 m/s in clean sands.

For sandy soils with $FC \geq 35\%$, the SPT-based chart by Seed et al. (1985) indicated a limiting upper $(N_1)_{60}$ value of about 21 for cyclic liquefaction occurrence. The correlation by Ohta and Goto (1978) suggested equivalent V_{S1} values of 195 m/s for Holocene sands. The stress-corrected cross-hole measurements compiled by Sykora (1987) for Holocene sands and nonplastic silty sands below the ground-water table with $(N_1)_{60}$ between 16 and 26 exhibited an average value of 199 m/s and standard deviation of 36 m/s. From these estimates, a V_{S1} value of 195 m/s is assumed equivalent to an $(N_1)_{60}$ value of 21 in soils with $FC \geq 35\%$.

To permit the CRR-V_{S1} curves for magnitude 7.5 earthquakes to have V_{S1} values between 195 and 210 m/s at CRR near 0.6, values of V_{S1}^* are assumed to range linearly from 200 to 215 m/s. The relationship between V_{S1}^* and fines content can be expressed by

$$V_{S1}^* = 215 \text{ m/s}, \quad \text{for sands with } FC \leq 5\% \tag{11a}$$

$$V_{S1}^* = 215 - 0.5(FC - 5) \text{ m/s}, \quad \text{for sands with } 5\% < FC < 35\% \tag{11b}$$

$$V_{S1}^* = 200 \text{ m/s}, \quad \text{for sands and silts with } FC \geq 35\% \tag{11c}$$

where FC = average fines content in percent by mass.

To illustrate how well the recommended CRR-V_{S1} curves defined by (7) and (11) fit the case history data, the data, separated by soil type, are presented in Figs. 7(a–d). The recommended curves provide reasonable bounds for all case history data above a CSR value of 0.35, indicating the use of the suggested V_{S1}^* values for sands and silts, as well as gravels. The use of these V_{S1}^* values for gravels is discussed below.

Curve-Fitting Parameters *a* and *b*

The three CRR-V_{S1} curves shown in Figs. 5 and 7 were determined through an iterative process of varying the values of a and b until nearly all case histories were bounded by the curves with the least amount of nonliquefaction case histories in the liquefaction region. The final values of a and b used to draw the curves were 0.022 and 2.8, respectively.

Of the 99 liquefaction case histories shown in Figs. 5 and

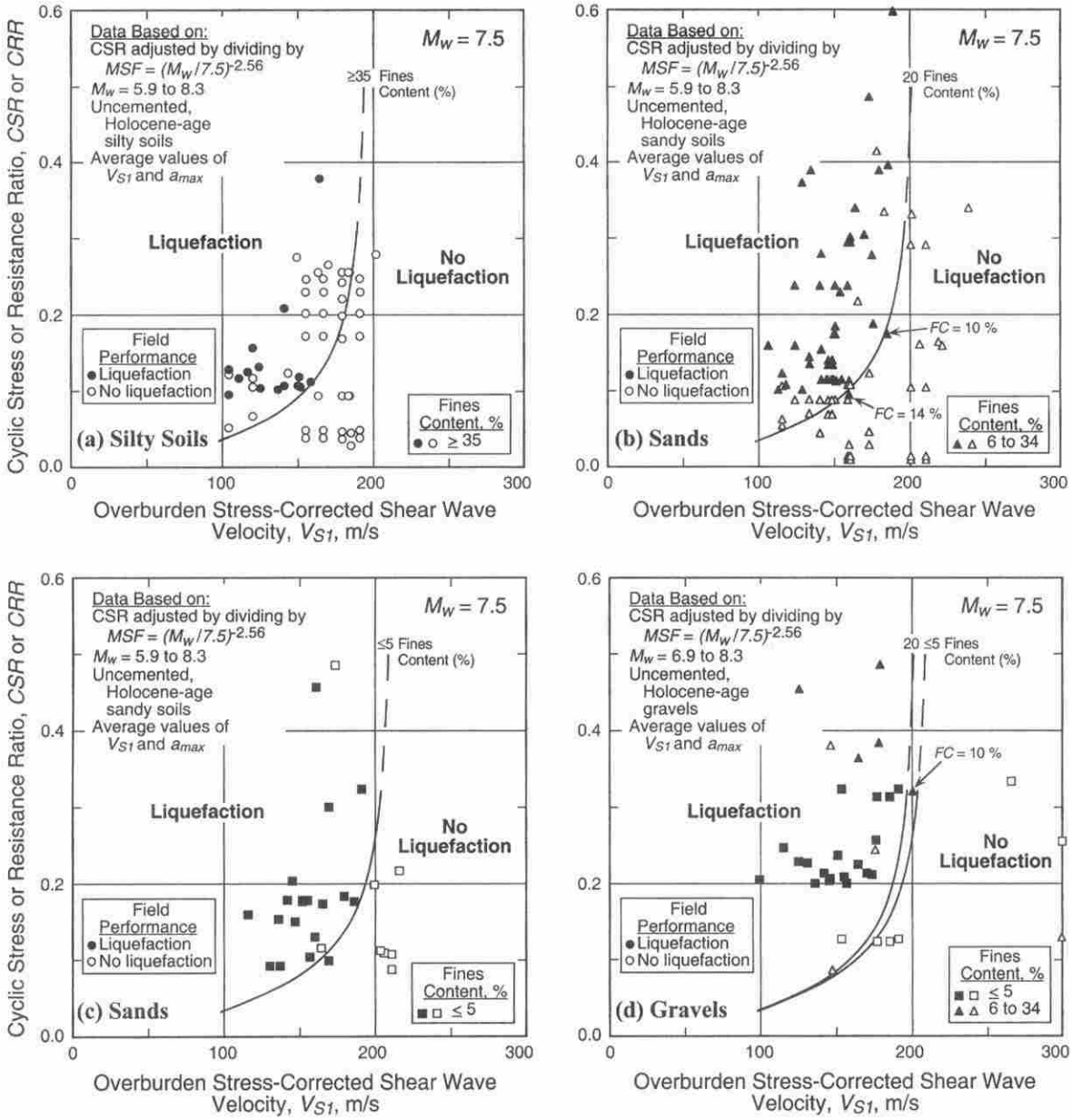

FIG. 7. Curves Recommended for Calculation of *CRR* from V_{s1} Measurements in Sands and Gravels along with Case History Data Separated by Soil Type

7, only two incorrectly lie in the No Liquefaction region. The two case histories that incorrectly lie in the No Liquefaction region are two sites at Treasure Island, Calif., where liquefaction was marginal during the 1989 Loma Prieta earthquake (M_w = 7). It is interesting to note that similar incorrect evaluations also are obtained when one uses the SPT data for these two sites (Andrus et al. 1999).

To illustrate the effect of using different values of *MSF* and r_d, the values of *CSR* for the case history data have been recalculated using the revised values of *MSF* and r_d proposed by Idriss (1999). The recalculated case history data are plotted in Fig. 8. Also plotted in Fig. 8 are the same three *CRR*-V_{S1} curves shown in Fig. 5. Many of the case history data in Fig. 8 plot at higher *CSR* values than in Fig. 5, because the earthquake magnitude is ≤7.5 for most of the data. The upward shift in the liquefaction data points near *CSR* of 0.1 is <0.01. This difference is not significant and is within the accuracy of the plotted data.

At magnitudes less than about 7, the difference in using values of *MSF* and r_d proposed by Idriss (1999) and those adopted by the NCEER workshop (Youd et al. 1997) is significant in the calculation of *CSR*. For M_w near 5.5, the differences in *CSR* are about 0.02 at V_{S1} = 100 m/s and 0.1 at V_{S1} at 200 m/s.

Limiting Upper Value of V_{s1} in Gravelly Soils

Although the V_{S1}^* values given in (11) were determined for sandy soils, the results presented in Fig. 7(d) indicate that these limits also represent reasonable limits for gravelly soils divided into the same categories based on fines content. This might be considered rather surprising based on the penetration-V_S correlations presented in the literature for gravelly soils. For instance, the correlation by Ohta and Goto (1978) suggested a V_{S1} value of 227 m/s for Holocene gravels at an equivalent $(N_1)_{60}$ of 30. Similarly, the correlation by Rollins et al. (1998) provided a best-fit V_{S1} value of 232 m/s for Holocene gravels. On the other hand, all the liquefaction case history data shown in Figs. 5 and 7 exhibit V_{S1} values of about 200 m/s or less, suggesting that 230 m/s may be inappropriately high. To investigate further the value of V_{S1}^* in gravelly soils, laboratory studies involving V_S measurements in gravelly

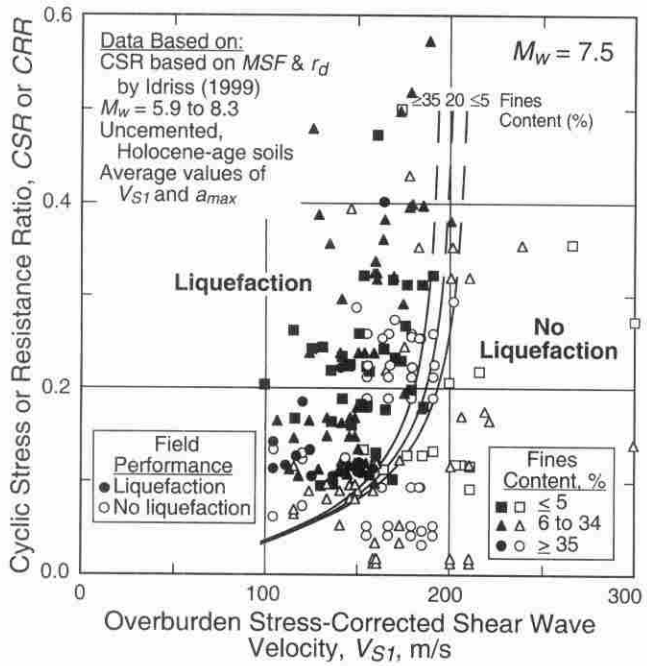

FIG. 8. Curves Recommended for Calculation of *CRR* from V_{S1} Measurements along with Case History Data Based on Revised Values of *MSF* and r_d Proposed by Idriss (1999)

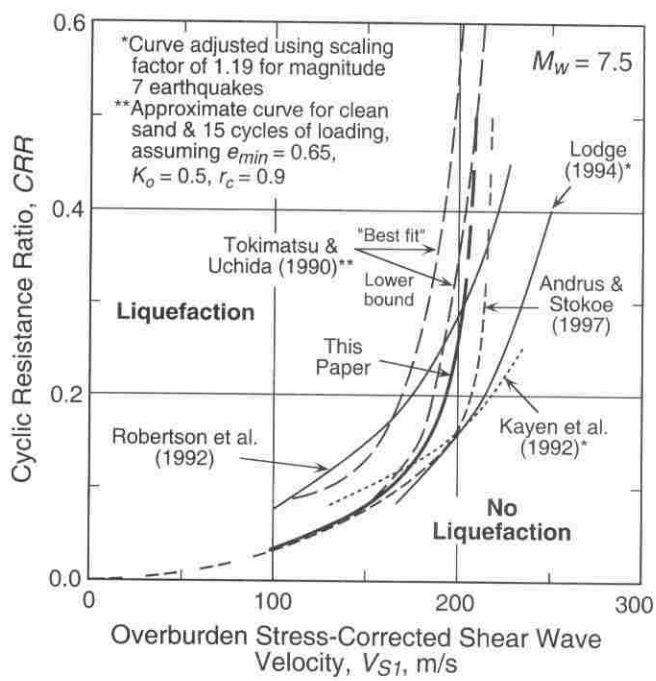

FIG. 9. Comparison of Seven Proposed *CRR*-V_{S1} Curves

soils were reviewed. Kokusho et al. (1995) clearly showed that the shear-wave velocity of gravelly soils varies greatly and is highly dependent on the particle gradation. Weston (1996) showed similar results for coarse sands with gravels. In both cases, the results show that increasing the uniformity coefficient can significantly increase the shear-wave velocity in medium-dense to dense gravels. On the other hand, very loose gravelly soils, even well-graded gravels, can exhibit shear-wave velocities similar to those of loose sands (Kokusho et al. 1995). The case history data presented in Fig. 7(d) support the premise that gravelly soils that are loose enough to exhibit significant liquefaction effects (boils, ground cracks, etc.) have shear-wave velocities similar to loose sands. Hence, the authors recommended the boundaries developed for sandy soils as preliminary boundaries for gravelly soils. However, additional work is clearly needed to understand the relationship between V_{S1} and liquefaction resistance of gravels.

Other *CRR*-V_{S1} Curves

Fig. 9 compares the *CRR*-V_{S1} curve for clean soils proposed in this paper with six other proposed *CRR*-V_{S1} curves. The best-fit curve by Tokimatsu and Uchida (1990) was determined using cyclic triaxial test results for various sands with <10% fines. It has been adjusted to be consistent with procedures outlined in this paper. The more conservative lower-bound curve for Tokimatsu and Uchida's data (determined by Andrus et al. 1999) also is shown in Fig. 9, because the other *CRR*-V_{S1} curves were drawn to bound liquefaction cases. The bounding curve by Robertson et al. (1992) was developed using field performance data from sites in Imperial Valley, Calif., and four other locations. To position their curve for magnitude 7.5 earthquakes, Robertson et al. used magnitude scaling factors similar to those suggested by Seed and Idriss (1982). Kayen et al. (1992) studied four sites that did and did not liquefy during the 1989 Loma Prieta earthquake. Lodge (1994) considered the same sites that Kayen et al. studied as well as a few other sites. The curve by Lodge was established by determining high or low liquefaction potential for each layer, using available SPT blow counts and the procedure of Seed et al. (1985). Values of V_{S1} and *CSR* were then plotted for both layer types. The bounding curves for Kayen et al. and Lodge shown in Fig. 9 have been adjusted for magnitude 7.5 earthquakes by assuming a *MSF* of 1.19, the lower-bound value for magnitude 7 earthquakes recommended by the 1996 NCEER workshop (Youd et al. 1997). The curve by Andrus and Stokoe (1997) was developed for the 1996 NCEER workshop, using case histories from 20 earthquakes.

As discussed by Andrus et al. (1999), many of the differences among the seven curves shown in Fig. 9 can be explained by the different levels of conservatism assumed with limited data and different methods used for selecting site variables and correction factors. Also, some errors were identified in the database by Andrus and Stokoe (1997). Thus, the *CRR*-V_{S1} curves proposed in this paper are recommended because they were based on the largest, most correct case history data set and procedures recommended by the 1996 NCEER workshop (Youd et al. 1997).

Recommended *CRR*-V_{S1} Curves

The recommended *CRR*-V_{S1} curves presented in Fig. 5 are defined by (7), (8), and (11) with $a = 0.022$, $b = 2.8$, $V_{S1}^* = 200–215$ m/s (depending on fines content), and $n = -2.56$. The value of -2.56 for n is recommended because it provides more conservative *CRR* values then -3.3, which is the n value defining the upper bound of the range of *MSF*s suggested by the 1996 NCEER workshop (Youd et al. 1997) for magnitudes <7.5. Although the *MSF*s defined by (8) with $n = -2.56$ provide less conservative curves than the factors proposed by Idriss (1999) for magnitudes <7.5, the findings of Ambraseys (1988), I. M. Idriss (personal communication, October 1995), Arango (1996), Youd and Noble (1997), Andrus and Stokoe (1997), and Andrus et al. (1999) supported their use.

The recommended curves shown in Fig. 5 are dashed above *CRR* of 0.35 to indicate that field performance data are limited. They do not extend much below 100 m/s, because there are no field data to support extending them to the origin. It is important to note that these boundary curves are for extreme behavior, where boils and ground cracks occur.

Correlation Between V_{S1} and $(N_1)_{60}$

One can obtain a correlation between V_{S1} and $(N_1)_{60}$ from the recommended *CRR*-V_{S1} relationships and 1996 NCEER

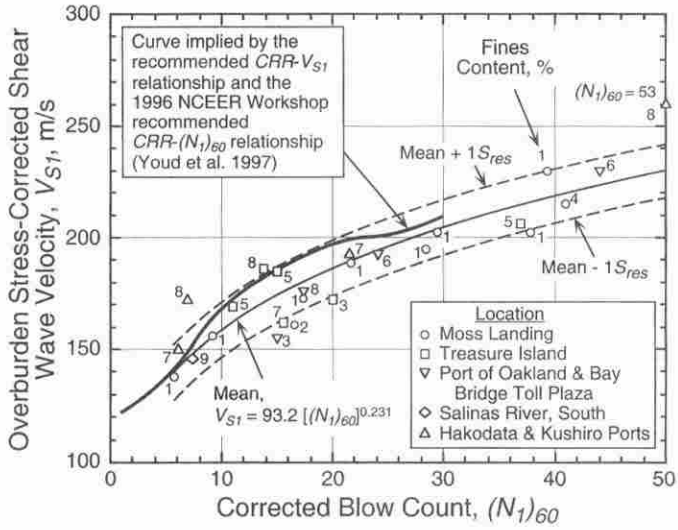

FIG. 10. Correlation between V_{S1} and $(N_1)_{60}$ for Clean Sands Implied by Recommended CRR-V_{S1} Relationship and 1996 NCEER Workshop Recommended CRR-$(N_1)_{60}$ Relationship (Youd et al. 1997) with Field Data for Sands with <10% Nonplastic Fines

workshop (Youd et al. 1997) recommended SPT-based relationship by plotting values with equal *CRR*. Fig. 10 presents the correlation of V_{S1} with $(N_1)_{60}$ for clean sands, based on the recommended *CRR*-V_{S1} and *CRR*-$(N_1)_{60}$ relationships. Also shown are the field data and mean curve for sands with <10% nonplastic fines from Fig. 6. The correlation derived from the *CRR* relationships lies between the mean and mean $+1S_{res}$ curves. Both V_{S1} and $(N_1)_{60}$-based liquefaction evaluation procedures provide similar predictions of liquefaction potential, when the data point lies on the *CRR*-based curve. When the data point plots below the *CRR*-based curve, the V_{S1}-based liquefaction evaluation procedure provides the more conservative prediction. When the data point plots above the *CRR*-based curve, the SPT-based procedure provides the more conservative prediction. Because most of the data points shown in Fig. 10 plot below the *CRR*-based curve, the V_{S1}-based procedure provides an overall more conservative prediction of liquefaction resistance than does the SPT-based procedure for these sites.

Factor of Safety

A common way to quantify the potential for liquefaction is in terms of a factor of safety. The factor of safety *FS* against liquefaction can be defined by

$$FS = \frac{CRR}{CSR} \tag{12}$$

Liquefaction is predicted to occur when $FS \leq 1$, and liquefaction is predicted not to occur when $FS > 1$. The acceptable value of *FS* will depend on several factors, including the acceptable level of risk for the project, potential for ground deformation, extent and accuracy of seismic measurements, availability of other site information, and conservatism in determining the design earthquake magnitude and expected value of a_{max}.

CORRECTION FACTORS

The recommended *CRR*-V_{S1} curves are limited to the characteristics of the database summarized earlier in this paper. Correction factors may be used to extend the curves to site conditions different from the database.

In areas of cemented and aged soils (>10,000 years), a correction factor can be added to (7) as follows:

$$CRR = \left\{ a \left(\frac{K_c V_{S1}}{100} \right)^2 + b \left(\frac{1}{V_{S1}^* - K_c V_{S1}} - \frac{1}{V_{S1}^*} \right) \right\} MSF \tag{13}$$

where K_c = correction factor for high values of V_{S1} caused by cementation and aging. Average estimates of K_c for Pleistocene-age soils range from 0.6 to 0.8 based on penetration-V_{S1} correlations (Ohta and Goto 1978; Rollins et al. 1998).

Fig. 11 illustrates a method for estimating the value of K_c using SPT blow counts. Shown in Fig. 11(a) are the V_{S1}-$(N_1)_{60}$ relationships for clean and silty sands implied by the recommended *CRR*-V_{S1} curves and 1996 NCEER workshop recommended *CRR*-$(N_1)_{60}$ curves (Youd et al. 1997). From these implied curves, the design curves shown in Fig. 11(b) were developed. In the example, the measured values of V_{S1}, $(N_1)_{60}$, and *FC* are 220 m/s, 8, and 10%, respectively. The relationships shown in Fig. 11(b) suggest a K_c value of 0.71 for these conditions. This method for estimating K_c assumes that the strain level induced during penetration testing is the same strain level causing liquefaction, which may not be true because pore-water pressure buildup to liquefaction can occur at medium strains in several loading cycles (Dobry et al. 1982; Seed et al. 1983). The method also assumes that liquefaction potential and blow count are not affected by cementation, which may not be a reasonable assumption. Hence, this suggested method should be used cautiously and with engineering judgment.

In soils above the ground-water table, particularly silty soils, negative pore pressures increase the effective state of stress and, hence, the value of V_S measured in seismic tests. This effect should be considered in the estimation of σ_v' for correcting V_S to V_{S1} and for computing *CSR* using (2).

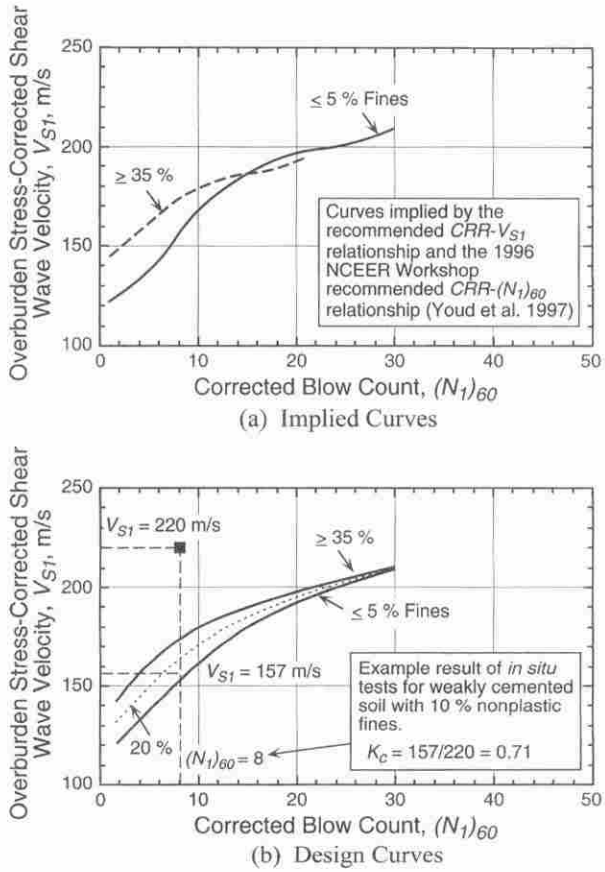

FIG. 11. Correlations between V_{S1} and $(N_1)_{60}$ Implied by Recommended CRR-V_{S1} Relationship and 1996 NCEER Workshop Recommended CRR-$(N_1)_{60}$ Relationship (Youd et al. 1997) with Example for Determining Correction Factor K_c at Weakly Cemented Soil Site

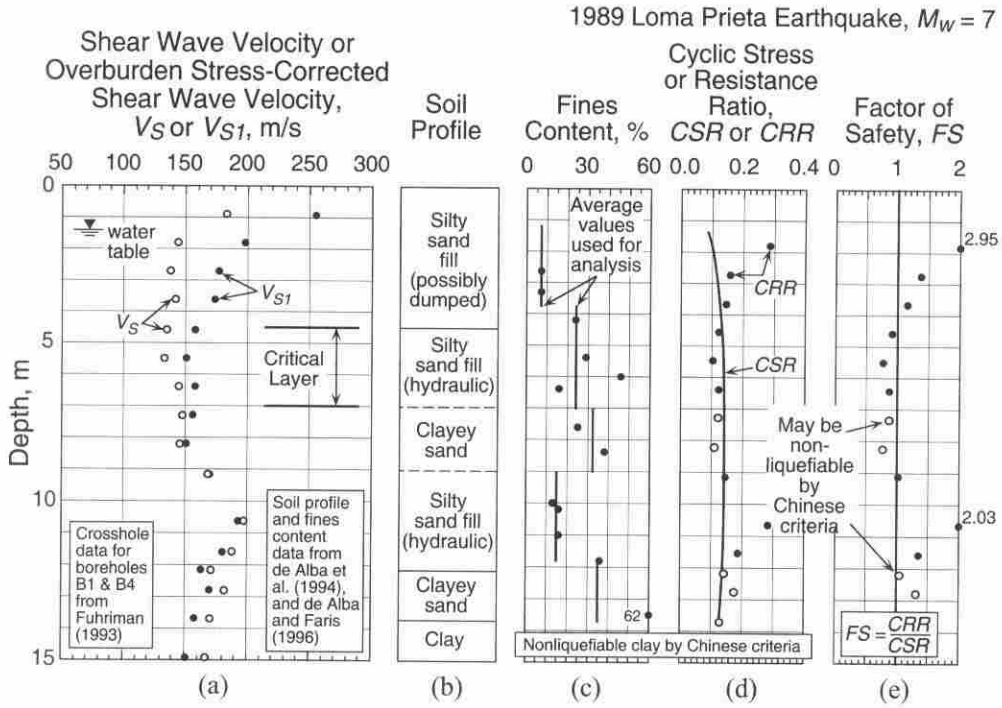

FIG. 12. Application of Recommended Procedure to Treasure Island Fire Station Site and 1989 Loma Prieta Earthquake

CASE STUDY

To illustrate the evaluation procedure, the liquefaction potential at the Treasure Island fire station site during the 1989 Loma Prieta earthquake is presented. In this case, values of V_S were measured by cross-hole testing. Values of V_S and *CSR* are shown in Figs. 12(a and d), respectively. These values were calculated assuming soil densities of 1.76 Mg/m^3 above the water table and 1.92 Mg/m^3 below the water table. Also assumed in the evaluation were the average values of r_d originally proposed by Seed and Idriss (1971). Based on peak values of 0.16g and 0.11g recorded in two horizontal directions at the fire station during the 1989 earthquake (Brady and Shakal 1994), a geometric mean value of 0.13g was assumed for a_{max}. Profiles of soil type and fines content shown in Figs. 12(b and c) were based on information provided by de Alba et al. (1994) and de Alba and Faris (1996). Values of *CRR* were calculated assuming an *MSF* value of 1.19, the lower-bound value recommended by the 1996 NCEER workshop (Youd et al. 1997). The value of K_c was assumed equal to 1, because the soil to be evaluated at this site was uncemented and <10,000 years old.

Values of *FS* shown in Fig. 12(e) are <1 for the depths of 4–9 m. Between the depths of 4 and 7 m, the sand contains nonplastic fines and is considered liquefiable. Between the depths of 7 and 9 m, the soil exhibits plastic characteristics and may not be nonliquefiable by the so-called Chinese criteria. According to the Chinese criteria, nonliquefiable clayey soils have clay contents (particles <5 μm) ≥15%, liquid limits ≥35%, or moisture contents ≤90% of the liquid limit (Seed and Idriss 1982). Thus, by the simplified V_S procedure, the layer predicted likely to liquefy, or the critical layer, lies between the depths of 4 and 7 m.

Although no sand boils or ground cracks occurred at the site during the 1989 earthquake (Bennett 1994), there was a sudden drop in the fire station strong ground motion recordings at about 15 s and small motion afterward (Idriss 1990). This behavior was unlike behavior observed in recordings at other seismograph stations located on soft-soil sites in the San Francisco Bay area. de Alba et al. (1994) attributed this behavior to liquefaction of an underlying sand. A similar sudden drop in the strong ground motion recordings occurred at the Port Island Downhole Array site in Kobe, Japan, during the 1995 Hyogo-ken Nanbu earthquake (Aguirre and Irikura 1997), where liquefaction and sand boils did occur. It is probable that the 4-m-thick layer capping the level-ground fire station site, predicted not to liquefy in Figs. 12(d and e), prevented the formation of sand boils at the ground surface (Ishihara 1985). Therefore, this case history confirms the V_S prediction method.

CONCLUSIONS

In this paper, a procedure is presented for evaluating liquefaction resistance through V_S measurements. The procedure can be summarized in the following 10 steps:

1. From available subsurface data, develop detailed profiles of V_S, soil type, fines content and, if possible, soil density and penetration resistance.
2. Identify the depth of the ground-water table, noting any seasonal fluctuations and artesian pressures.
3. Calculate the values of σ_v and σ'_v for each measurement depth at which seismic testing has been performed.
4. Correct the V_s measurements to the reference overburden stress of 100 kPa using (4). The correction factor C_V is limited to a maximum value of 1.4 at shallow depths.
5. Determine the value of V^*_{S1} for each measurement depth using (11), which is recommended for sandy as well as gravelly soils. If the fines content is unknown, assume 215 m/s.
6. Determine the value of K_c. The value of K_c can be assumed equal to 1 if the soil to be evaluated is uncemented and <10,000 years old. If the soil conditions are unknown and penetration data are not available, assume 0.6 for K_c.
7. Determine the design earthquake magnitude and expected value of a_{max}.
8. Calculate *CSR* for each measurement depth below the water table using (2). The value of r_d can be estimated

from the average curve originally proposed by Seed and Idriss (1971).

9. Plot values of V_{S1} and *CSR* and appropriate liquefaction resistance curves defined by (8), (11), and (13), with $a = 0.022$, $b = 2.8$, and $n = -2.56$.
10. Calculate the value of *FS* for each measurement depth using (12). Liquefaction is predicted to occur when $FS \leq 1$. Liquefaction is predicted not to occur when $FS > 1$.

The procedure should be used cautiously and with engineering judgment when applying it to sites where conditions are different from the database. The case history data, and *CRR*-V_{S1} curves, are limited to relatively level ground sites with average depths <10 m, uncemented soils of Holocene age, ground-water table depths between 0.5 and 6 m, and V_S measurements performed below the water table.

Three concerns when using V_S as an indicator of liquefaction resistance are (1) its higher sensitivity (when compared with the penetration-based methods) to weak interparticle bonding; (2) the lack of a physical sample for identifying nonliquefiable clayey soils; and (3) not detecting thin liquefiable strata because the test interval is too large. The preferred practice when using V_S measurements to evaluate liquefaction resistance is to drill sufficient boreholes and conduct sufficient in situ tests to detect liquefiable weakly cemented soils, identify nonliquefiable clay-rich soils, and delineate thin liquefiable strata.

ACKNOWLEDGMENTS

Much of the work presented in this paper was funded by the National Institute of Standards and Technology (NIST), Gaithersburg, Md. The writers gratefully acknowledge the support and encouragement of Riley Chung, formerly with NIST, and Nicholas Carino at NIST. They thank the 1996 NCEER and 1998 MCEER workshop participants for their valuable reviews of this work, in particular, Gonzalo Castro of GEI Consultants, Winchester Mass., Ricardo Dobry of the Rensselaer Polytechnic Institute, Troy, N.Y., Mary Ellen Hynes of the U.S. Army Corps of Engineers, I. M. Idriss of the University of California at Davis, Maurice S. Power of Geomatrix Consultants, Oakland, Calif., Peter K. Robertson of the University of Alberta, and T. Leslie Youd of Brigham Young University, Provo, Utah. Also, special thanks go to Susumu Iai and Kohji Ichii of the Port and Harbour Research Institute, Yokosuka, Japan, Osamu Matsuo of the Public Works Research Institute, Tsukuba City, Japan, Susumu Yasuda of Tokyo Denki University, Hatoyama, Japan, Mamoru Kanatani and Yukihisa Tanaka of the Central Research Institute for Electric Power Industry, Abiko, Japan, Kohji Tokimatsu of the Tokyo Institute of Technology, and Takeji Kokusho of Chuo University, Tokyo, for the information on Japanese liquefaction studies graciously shared with the first writer. Michael Bennett of the U.S. Geological Survey, Ross Boulanger of the University of California at Davis, and Roman Hryciw of the University of Michigan, Ann Arbor, Mich., provided information on several California liquefaction studies. David Sykora of Bing Yen & Associates, Irvine, Calif., kindly shared his database of V_S measurements and SPT blow counts. The review comments of Richard Woods of the University of Michigan, Ann Arbor, Mich., as well as the anonymous reviewers, also are sincerely appreciated.

APPENDIX I. REFERENCES

Aguirre, J., and Irikura, K. (1997). "Nonlinearity, liquefaction, and velocity variation of soft soil layers in Port Island, Kobe, during the Hyogo-ken Nanbu earthquake." *Bull. Seismological Soc. of Am.*, 87(5), 1244–1258.

Ambraseys, N. N. (1988). "Engineering seismology." *Earthquake Engrg. and Struct. Dyn.*, 17, 1–105.

Andrus, R. D., and Stokoe, K. H., II. (1997). "Liquefaction resistance based on shear wave velocity." *Proc., NCEER Workshop on Evaluation of Liquefaction Resistance of Soils, Tech. Rep. NCEER-97-0022*, T. L. Youd and I. M. Idriss, eds., National Center for Earthquake Engineering Research, Buffalo, 89–128.

Andrus, R. D., Stokoe, K. H., II, and Chung, R. M. (1999). "Draft guidelines for evaluating liquefaction resistance using shear wave velocity measurements and simplified procedures." *NISTIR 6277*, National Institute of Standards and Technology, Gaithersburg, Md.

Arango, I. (1996). "Magnitude scaling factors for soil liquefaction evaluations." *J. Geotech. Engrg.*, ASCE, 122(11), 929–936.

Belloti, R., Jamiolkowski, J., Lo Presti, D. C. F., and O'Neill, D. A. (1996). "Anisotropy of small strain stiffness of Ticino sand." *Géotechnique*, London, 46(1), 115–131.

Bennett, M. (1994). "Subsurface investigation for liquefaction analysis and piezometer calibration at Treasure Island Naval Station, California." *Open File Rep. 94-709*, U.S. Geological Survey, Menlo Park, Calif.

Bierschwale, J. G., and Stokoe, K. H., II. (1984). "Analytical evaluation of liquefaction potential of sands subjected to the 1981 Westmorland earthquake." *Geotech. Engrg. Report 95-663*, University of Texas, Austin, Tex.

Boulanger, R. W., Mejia, L. H., and Idriss, I. M. (1997). "Liquefaction at Moss Landing during Loma Prieta earthquake." *J. Geotech. and Geoenvir. Engrg.*, ASCE, 123(5), 453–467.

Brady, A. G., and Shakal, A. F. (1994). "Strong-motion recordings." *The Loma Prieta, Calif., Earthquake of Oct. 17, 1989—Strong Ground Motion, U.S. Geological Survey Profl. Paper 1551-A*, R. D. Borcherdt, ed., U.S. Government Printing Office, Washington, D.C., A9–A38.

de Alba, P., Baldwin, K., Janoo, V., Roe, G., and Celikkol, B. (1984). "Elastic-wave velocities and liquefaction potential." *Geotech. Testing J.*, 7(2), 77–87.

de Alba, P., Benoît, J., Pass, D. G., Carter, J. J., Youd, T. L., and Shakal, A. F. (1994). "Deep instrumentation array at the Treasure Island Naval Station." *The Loma Prieta, Calif., Earthquake of Oct. 17, 1989—Strong Ground Motion, U.S. Geological Survey Profl. Paper 1551-A*, R. D. Borcherdt, ed., U.S. Government Printing Office, Washington, D.C., A155–A168.

de Alba, P., and Faris, J. R. (1996). "Workshop on future research deep instrumentation array, Treasure Island NGES, July 27, 1996." *Rep. to the Workshop, Current State of Site Characterization and Instrumentation*, University of New Hampshire, Durham, N.H.

Dobry, R. (1989). "Some basic aspects of soil liquefaction during earthquakes." *Earthquake hazards and the design of constructed facilities in the eastern United States, Ann. of the New York Acad. of Sci.*, K. H. Jacob and C. J. Turkstra, eds., New York, 558, 172–182.

Dobry, R., Ladd, R. S., Yokel, F. Y., Chung, R. M., and Powell, D. (1982). "Prediction of pore water pressure buildup and liquefaction of sands during earthquakes by the cyclic strain method." *NBS Build. Sci. Ser. 138*, National Bureau of Standards, Gaithersburg, Md.

Dobry, R., Stokoe, K. H., II, Ladd, R. S., and Youd, T. L. (1981). "Liquefaction susceptibility from S-wave velocity," *Proc., ASCE Nat. Convention, In Situ Tests to Evaluate Liquefaction Susceptibility*, ASCE, New York.

Fuhriman, M. D. (1993). "Crosshole seismic tests at two northern California sites affected by the 1989 Loma Prieta earthquake." MS thesis, University of Texas, Austin, Tex.

Golesorkhi, R. (1989). "Factors influencing the computational determination of earthquake-induced shear stresses in sandy soils." PhD dissertation, University of California, Berkeley, Calif.

Hardin, B. O., and Drnevich, V. P. (1972). "Shear modulus and damping in soils: Design equations and curves." *J. Soil Mech. and Found. Div.*, ASCE, 98(7), 667–692.

Idriss, I. M. (1990). "Response of soft soil sites during earthquakes." *Proc., H. B. Seed Memorial Symp.*, Vol. 2, BiTech Publisher, Vancouver, 273–289.

Idriss, I. M. (1999). "Presentation notes: An update of the Seed-Idriss simplified procedure for evaluating liquefaction potential." *Proc., TRB Workshop on New Approaches to Liquefaction Anal., Publ. No. FHWA-RD-99-165*, Federal Highway Administration, Washington, D.C.

Ishihara, K. (1985). "Stability of natural deposits during earthquakes." *Proc., 11th Int. Conf. on Soil Mech. and Found. Engrg.*, Balkema, Rotterdam, The Netherlands, 321–376.

Jamiolkowski, M., and Lo Presti, D. C. F. (1990). "Correlation between liquefaction resistance and shear wave velocity." *Soils and Found.*, Tokyo, 32(2), 145–148.

Kayen, R. E., Mitchell, J. K., Seed, R. B., Lodge, A., Nishio, S., and Coutinho, R. (1992). "Evaluation of SPT-, CPT-, and shear wave-based methods for liquefaction potential assessment using Loma Prieta data." *Proc., 4th Japan-U.S. Workshop on Earthquake Resistant Des. of Lifeline Fac. and Countermeasures for Soil Liquefaction, Tech. Rep. NCEER-92-0019*, M. Hamada and T. D. O'Rourke, eds., Vol. 1, National Center for Earthquake Engineering Research, Buffalo, 177–204.

Kokusho, T., Yoshida, Y., and Tanaka, Y. (1995). "Shear wave velocity in gravelly soils with different particle gradings." *Static and dynamic properties of gravelly soils, Geotech. Spec. Publ. No. 56*, M. D. Evans and R. J. Fragaszy, eds., ASCE, New York, 92–106.

Lodge, A. L. (1994). "Shear wave velocity measurements for subsurface characterization." PhD dissertation, University of California, Berkeley, Calif.

Ohta, Y., and Goto, N. (1978). "Physical background of the statistically

obtained S-wave velocity equation in terms of soil indexes." *Butsuri-Tanko (Geophys. Exploration)*, Tokyo, 31(1), 8–17 (in Japanese).
Olsen, R. S. (1997). "Cyclic liquefaction based on the cone penetrometer test." *Proc., NCEER Workshop on Evaluation of Liquefaction Resistance of Soils, Tech. Rep. NCEER-97-0022*, T. L. Youd and I. M. Idriss, eds., National Center for Earthquake Engineering Research, Buffalo, 225–276.
Robertson, P. K., and Campanella, R. G. (1985). "Liquefaction potential of sands using the CPT." *J. Geotech. Engrg.*, ASCE, 111(3), 384–403.
Robertson, P. K., Woeller, D. J., and Finn, W. D. L. (1992). "Seismic cone penetration test for evaluating liquefaction potential under cyclic loading." *Can. Geotech. J.*, Ottawa, 29, 686–695.
Robertson, P. K., and Wride, C. E. (1998). "Evaluating cyclic liquefaction potential using the cone penetration test." *Can. Geotech. J.*, Ottawa, 35(3), 442–459.
Roesler, S. K. (1979). "Anisotropic shear modulus due to stress anisotropy." *J. Geotech. Engrg. Div.*, ASCE, 105(7), 871–880.
Rollins, K. M., Evans, M. D., Diehl, N. B., and Daily, W. D., III. (1998). "Shear modulus and damping relationships for gravels." *J. Geotech. and Geoenvir. Engrg.*, ASCE, 124(5), 396–405.
Roy, D., Campanella, R. G., Byrne, P. M., and Hughes, J. M. O. (1996). "Strain level and uncertainty of liquefaction related index tests." *Uncertainty in the geologic environment: From theory to practice, Geotech. Spec. Publ. No. 58*, Vol. 2, C. D. Shackelford, P. P. Nelson, and M. J. S. Roth, eds., ASCE, New York, 1149–1162.
Seed, H. B. (1979). "Soil liquefaction and cyclic mobility evaluation for level ground during earthquakes." *J. Geotech. Engrg. Div.*, ASCE, 105(2), 201–255.
Seed, H. B., and de Alba, P. (1986). "Use of SPT and CPT tests for evaluating the liquefaction resistance of sands." *Use of in situ tests in geotechnical engineering, Geotech. Spec. Publ. No. 6*, ASCE, New York, 1249–1273.
Seed, H. B., and Idriss, I. M. (1971). "Simplified procedure for evaluating soil liquefaction potential." *J. Soil Mech. and Found. Div.*, ASCE, 97(9), 1249–1273.
Seed, H. B., and Idriss, I. M. (1982). *Ground motions and soil liquefaction during earthquakes*, Earthquake Engineering Research Institute, Berkeley, Calif.
Seed, H. B., Idriss, I. M., and Arango, I. (1983). "Evaluation of liquefaction potential using field performance data." *J. Geotech. Engrg.*, ASCE, 109(3), 458–482.
Seed, H. B., Tokimatsu, K., Harder, L. F., and Chung, R. M. (1985). "The influence of SPT procedures in soil liquefaction resistance evaluations." *J. Geotech. Engrg.*, ASCE, 111(12), 1425–1445.
Stark, T. D., and Olson, S. M. (1995). "Liquefaction resistance using CPT and field case histories." *J. Geotech. Engrg.*, ASCE, 121(12), 856–869.
Stokoe, K. H., II, Lee, S. H. H., and Knox, D. P. (1985). "Shear moduli measurements under true triaxial stresses." *Proc., Adv. in the Art of Testing Soil Under Cyclic Conditions*, ASCE, New York, 166–185.
Stokoe, K. H., II, and Nazarian, S. (1985). "Use of Rayleigh waves in liquefaction studies." *Measurement and use of shear wave velocity for evaluating dynamic soil properties*, R. D. Woods, ed., ASCE, New York, 1–17.
Stokoe, K. H., II, Nazarian, S., Rix, G. J., Sanchez-Salinero, I., Sheu, J.-C., and Mok, Y. J. (1988a). "In situ seismic testing of hard-to-sample soils by surface wave method." *Earthquake engineering and soil dynamics II—Recent advances in ground-motion evaluation, Geotech. Spec. Publ. No. 20*, J. L. Von Thun, ed., ASCE, New York, 264–289.
Stokoe, K. H., II, Roësset, J. M., Bierschwale, J. G., and Aouad, M. (1988b). "Liquefaction potential of sands from shear wave velocity." *Proc., 9th World Conf. on Earthquake Engrg.*, Vol. III, 213–218.
Sykora, D. W. (1987). "Creation of a data base of seismic shear wave velocities for correlation analysis." *Geotech. Lab. Miscellaneous Paper GL-87-26*, U.S. Army Engineer Waterways Experiment Station, Vicksburg, Miss.
Teachavorasinskun, S., Tatsuoka, F., and Lo Presti, D. C. F. (1994). "Effects of the cyclic prestaining on dilatancy characteristics and liquefaction strength of sand." *Pre-failure deformation of geomaterials*, S. Shibuya, T. Mitachi, and S. Miura, eds., Balkema, Rotterdam, The Netherlands, 75–80.
Tokimatsu, K., and Uchida, A. (1990). "Correlation between liquefaction resistance and shear wave velocity." *Soils and Found.*, Tokyo, 30(2), 33–42.
U.S. Bureau of Reclamation (USBR). (1989). "Seismic design and analysis." Chapter 13, *Design Standards No. 13—Embankment Dams*, Denver, Colo., 28–29.
Weston, T. R. (1996). "Effects of grain size and particle distribution on the stiffness and damping of granular soils at small strains." MS thesis, University of Texas, Austin, Tex.
Woods, R. D., ed. (1994). *Geophysical characterization of sites*, Balkema, Rotterdam, The Netherlands.
Youd, T. L., et al. (1997). "Summary report." *Proc., NCEER Workshop on Evaluation of Liquefaction Resistance of Soils, Tech. Rep. NCEER-97-0022*, T. L. Youd and I. M. Idriss, eds., National Center for Earthquake Engineering Research, Buffalo, 1–40.
Youd, T. L., and Noble, S. K. (1997). "Liquefaction criteria based on statistical and probabilistic analyses." *Proc., NCEER Workshop on Evaluation of Liquefaction Resistance of Soils, Tech. Rep. NCEER-97-0022*, T. L. Youd and I. M. Idriss, eds., National Center for Earthquake Engineering Research, Buffalo, 201–215.

APPENDIX II. NOTATION

The following symbols are used in this paper:

A = parameter that depends on soil structure;
a, b = parameter related to slope of CRR-V_{S1} curve;
a_{max} = peak horizontal ground surface acceleration;
B_1, B_2 = parameters relating V_{S1} and $(N_1)_{60}$;
CRR = average cyclic resistance ratio;
CSR = cyclic stress ratio;
C_V = overburden stress correction factor;
e_{min} = minimum void ratio;
FC = fines content (particles <75 μm);
FS = factor of safety;
$f(\gamma_{av})$ = function of average peak cyclic shear strain;
G_{max} = small-strain shear modulus;
$(G)_{\gamma_{av}}$ = secant shear modulus at γ_{av};
g = acceleration of gravity;
K_c = cementation and aging correction factor;
K_0' = coefficient of effective lateral earth pressure at rest;
MSF = magnitude scaling factor;
M_w = earthquake moment magnitude;
m = stress exponent;
$(N_1)_{60}$ = SPT energy-corrected and overburden stress-corrected blow count;
n = magnitude scaling factor exponent;
P_L = probability of liquefaction occurrence;
P_a = reference overburden stress (=100 kPa);
r_c = multidirectional shaking correction factor;
r_d = shear stress reduction coefficient;
S_{res} = residual standard deviation;
V_S = small-strain shear wave velocity;
V_{S1}^* = limiting upper value of V_{S1} for cyclic liquefaction occurrence;
V_{S1} = overburden stress-corrected V_S;
z = depth;
γ_{av} = average peak cyclic shear strain;
ρ = mass density of soil;
σ_h' = initial effective horizontal stress;
σ_v = total vertical (or overburden) stress;
σ_v' = initial effective vertical (or overburden) stress; and
τ_{av} = average cyclic equivalent uniform shear stress generated by earthquake.